CHAPTER 2: Regulation of protein content and composition in tobacco leaves through cysteine proteases

Submitted to Journal of Experimental Botany (in press): Prins, A., Van Heerden, P.D.R., Olmos, E., Kunert, K.J., Foyer, C.H. Cysteine proteases regulate chloroplast protein content and composition in tobacco leaves through interactions with ribulose-1,5-bisphosphate carboxylase/oxygenase (RuBiSCO) vesicular bodies.

2.1 Abstract

In light of previous results indicating that the exogenous expression of a rice cysteine protease inhibitor, OC-I, has a protective effect under low temperature stress (Van der Vyver et al, 2003), the mechanism by which this is affected was investigated in this part of the study. In particular, the roles of cysteine proteases (CP) in leaf protein accumulation and composition were investigated in transgenic tobacco plants expressing OC-I. The OC-I protein was present largely in the cytosol of the leaves of OC-I expressing (OCE) plants with small amounts associated with the chloroplasts and vacuole. Changes in leaf protein composition and turnover caused by OC-I-dependent inhibition of CP activity were assessed in young (6-8 week old) plants in a preliminary proteomic analysis. Seven hundred and sixty five soluble proteins were detected in the controls compared to 860 proteins in the OCE leaves at this stage. A cyclophilin, a histone, a peptidyl-prolyl cis-trans isomerase and two ribulose-, 5-bisphosphate carboxylase/oxygenase (RuBisCO) activase isoforms were markedly altered in abundance in the OCE leaves. Western blot analysis of plants after flowering revealed large increases in the amount of RuBisCO protein in the OCE leaves. The senescence-related decline in photosynthesis was delayed in the OCE leaves. Similarly, OCE leaves maintained higher leaf RuBisCO activities and protein than controls following exposure to dark chilling. Immunogold labelling studies with specific antibodies revealed that RuBisCO was present in RuBisCO vesicular bodies (RVBs) as well as in the chloroplasts of leaves from 8-week old control and OCE plants. The data presented here demonstrate that that CPs are involved in RuBisCO turnover in all leaves under optimal and stress conditions and that this process could involve interactions with RVBs.

2.2 Introduction

Cysteine proteases (CP) are involved with a variety of proteolytic functions in higher plants (Granell et al., 1998), particularly those associated with the processing and degradation of seed storage proteins (Shimada et al., 1994; Toyooka et al., 2000), and fruit ripening (Alonso and Granell, 1995). They are also induced in response to stresses, such as wounding, cold and drought (Schaffer and Fischer, 1988; Koizumi et al., 1993; Linthorst et al., 1993; Harrak et al., 2001), and in programmed cell death (Solomon et al., 1999; Xu and Chye, 1999). Like their CP targets, phytocystatins are regulated by developmental (Lohman et al., 1994) and environmental cues (Botella et al., 1996; Belenghi et al., 2003; Pernas et al., 2000; Diop et al., 2004).

Cysteine proteases have also been identified in tobacco, including a KDEL-type CP *Nt*CP2 (Beyene et al., 2006). The C-terminal KDEL motif, present in some cysteine proteases, is an endoplasmic reticulum retention signal for soluble proteins that allows CP propeptides to be stored either in a special organelle, called the ricinosome (Schmid et al., 1999), or in KDEL vesicles (KV) before transport to vacuoles through a Golgi complex-independent route (Okamoto et al., 2003). The relatively acidic pH optima of many of the endogenous plant CPs indicate that they are localized in the vacuole (Callis, 1995). A papain-like sequence, termed *Nt*CP1, has also been isolated from senescent tobacco leaves (Beyene et al., 2006). Papain-like cysteine proteases are often found in senescing organs particularly leaves (Lohman et al., 1994; Ueda et al., 2000; Gepstein et al., 2003), flowers (Eason et al., 2002), legume nodules (Kardailsky and Brewin, 1996) as well as in germinating seeds (Ling et al., 2003). Senescence -associated genes (SAGs) are up-regulated during leaf senescence (Lohman et al., 1994; Quirino et al., 1999; Swidzinski et al., 2002; Gepstein et al., 2003; Bhalerao et al., 2003; Lin and Wu, 2004). Of these the SAG12 cysteine protease is one of the very few SAGs that are highly senescence-specific (Lohman et al., 1994). While it is known that the major light-harvesting chlorophyll a/b protein of photosystem II as well as RuBisCO large subunit (LSU) is sensitive to degradation by cysteine proteases, the mechanism by which this occurs is unknown. Furthermore, it's unknown whether other chloroplast-located proteins are sensitive to cysteine protease-mediated degradation.

The expression of many photosynthesis genes such as those encoding the chlorophyll a/b binding protein and the ribulose-1, 5-bisphosphate carboxylase-oxygenase (RuBisCO)

subunits decreases during senescence and are hence classed as senescence down-regulated genes (Humbeck et al., 1996). RuBisCO degradation can occur both inside and outside the chloroplast (Irving and Robinson, 2006). Inside the chloroplast, oxidation of critical cysteine residues on the RuBisCO protein modifies the proteolytic susceptibility of these or associated amino acids, causing the protein to adhere to the chloroplast envelope and "marking" the protein for degradation (Garcia-Ferris and Moreno, 1994). Recent evidence suggests that the 26S proteasome is activated by carbonylation and hence this protein degradation pathway is enhanced when the cellular environment becomes even mildly oxidizing (Basset et al., 2002). In the chloroplast RuBisCO is protected against degradation by 2-carboxyarabinitol 1-phosphate (CA-1-P) but how this modulates degradation outside the chloroplast is unknown (Khan et al., 1999).

Little information is further available on the effects of ectopic phytocystatin expression on plant growth and development (Masoud et al., 1993; Guttiérrez-Campos et al., 2001; Van der Vyver et al., 2003) as most studies have concentrated on effects on insect resistance or protein production (Christou et al., 2006; Rivard et al., 2006). The phenotype resulting from expression of the rice cystatin, OC-I, in transformed tobacco plants has been described previously (Masoud et al., 1993; Guttiérrez-Campos et al., 2001; Van der Vyver et al., 2003). However, increased biomass production resulting from cystatin expression under field conditions is often attributed to enhanced insect resistance rather than to direct effects of the cystatin on endogenous protein turnover in the plant tissues. It has been shown that the transgenic OC-I expressing tobacco lines (OCE) grow more slowly with an extended vegetative phase compared to the wild type or empty vector controls (Van der Vyver et al., 2003). They are also more resistant to dark chilling-induced inhibition of photosynthesis (Van der Vyver et al., 2003). The following study was undertaken in order to determine how the constitutive expression of the rice cystatin, OC-I, in the cytosol of tobacco leaves alters leaf protein content and composition and exerts effects on photosynthesis in leaves at different stages of development. Furthermore, the possible sensitivity of RuBisCO to degradation by CP was investigated.

2.3 Materials and Methods

All methods were performed by A. Prins, unless otherwise indicated.

2.3.1 Plant material and growth conditions

Seeds of wild-type non-transformed tobacco (*Nicotiana tabacum* L. cv. Samsun), and a self-fertilized transformed tobacco OCE line (T4/5; Van der Vyver et al., 2003) expressing the gene encoding oryzacystatin-I (OC-I) and the β-glucuronidase coding sequence (*gus* gene) under the control of the 35S promoter, were germinated in trays with commercial peat/loam compost as described for maize plants (Chapter 2). Individual seedlings were transferred to small pots at 4-leaf stage and grown in controlled environment chambers in air. The plants were grown with a 15-h photoperiod at a light intensity of 800 - 1000µmol m^{-2} s^{-1} (at leaf level) with a day/night temperature of 26°C/20°C, and 80% (v/v) relative humidity (Fig. 2.1). When the roots started to appear at the base of the small pots, the plants were transferred to 8.5l volume (25cm diameter) pots. They were then grown to maturity (13 weeks; 20-28 leaf stage depending on the genotype). Plants were irrigated twice daily and maintained in water-replete conditions throughout. Samples were harvested for assay at various stages of development as indicated in the text and figure legends.

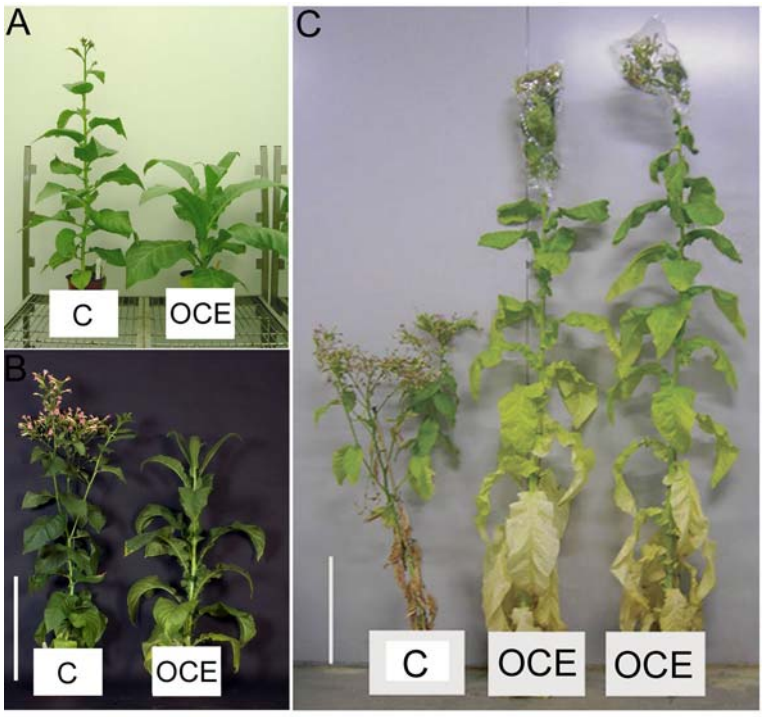

Figure 2.1 Wild type (C) and OC-I expressing (OCE) phenotypes at different developmental stages. Plants are shown at the following stages: A) 8 weeks, B) 10 weeks, and C) 14 weeks. Scale bar represents 0.5m.

2.3.2 Histochemical staining for GUS activity

Young transgenic tobacco plants (approximately 4 weeks old) were screened for transgene expressions using the GUS histochemical assay. Plant leaf tissue was incubated at 37ºC overnight in GUS-staining solution [1mg ml^{-1} 5-bromo-4-chloro-3-indolyl glucoronide in 50mM NaH_2PO_4 buffer, pH7 containing 0.01% (v/v) Tween 80 and 10mM Na_2EDTA]. Transformed plants posess the β-glucuronidase coding sequence (*gus* gene), which produces the hydrolase GUS. This enzyme catalyses the cleavage of 5-bromo-4-chloro-3-indolyl glucoronide, leading to a blue precipitate. Only plants showing expression of the *gus* gene were selected for further investigation.

2.3.3 Chilling treatments

The chilling treatment was performed by P.D.R van Heerden (Potchefstroom University), with leaf samples from plants exposed to chilling treatment being used by A. Prins for further analysis. Six week-old OCE and wild-type plants were subjected to chilling stress (5°C) in darkness for seven consecutive nights. At the end of each photoperiod, six transformed and wild type plants (from batches of 12 each) were transferred to a refrigerated chamber controlled at 5ºC for one entire dark period. The remaining six plants (controls) were kept under normal conditions in the growth chamber at 20ºC and represented the control treatment. Only the shoots and leaves of plants were dark chilled. The roots were kept at 20ºC during dark chilling by inserting the pots into custom designed pot-incubators (Analytical Scientific Instruments, Weltevreden Park, South Africa) that circulated warm air around the pots. This minimised the occurrence of chill-induced drought stress and associated leaf wilting which is a potential artifact that could interfere with interpretations based on the effects of dark chilling *per se* (Allen and Ort, 2001). After nine hours exposure to chilling, the treated plants were returned to the growth chamber where they remained throughout the 15h light period. This process was repeated for seven consecutive dark periods.

2.3.4 Growth analysis

The following measurements were performed at 13-14 weeks. In all experiments leaf phylogeny was classified from the base to the top of the stem, leaf one being at the bottom and leaf twelve at the top. Measurements were performed sequentially as follows:

i) Stem height

Stem height was measured from the base to the top of the stem with a ruler.

ii) Numbers of leaves

Leaves were counted from leaf 1 to 30.

iii) Leaf weight and area

The fresh weight and area of each leaf was measured following excision. Total leaf fresh weights were determined on a standard laboratory balance. Leaf area was measured using a ΔT area meter (Delta-T Devices LTD, England) according to instructions of the manufacturer.

iv) Days to flowering

The flowers were tagged at anthesis. Time to flowering is denoted as time taken for the first flower to open.

2.3.5 Photosynthesis measurements

Photosynthesis measurements were performed by P.D.R. van Heerden (Potchefstroom University). Photosynthetic gas exchange measurements were performed on attached leaves essentially as described in Novitskaya et al. (2002) and Van Heerden et al. (2003). CO_2 assimilation was measured every day after each of the dark chilling treatments on four individual plants of both the control and dark chilling treatments. Measurements were taken with an open circuit infrared gas analysis system (CIRAS-I, PP-systems, Herts, UK) in a 2.5cm^2 cuvette with built-in light and temperature control. Humidity in the cuvette was maintained close to ambient conditions. All measurements were started 3 h after the end of each dark period and conducted at 28°C. CO_2 assimilation at ambient growth conditions was measured at an irradiance of 350µmol m^{-2} s^{-1} and CO_2 (Ca) flow rate of 350µmol mol^{-1}. For the measurement of the relationship between CO_2 assimilation rate (A) and intercellular CO_2 concentration (Ci), irradiance in the leaf cuvette was controlled at 1250µmol m^{-2} s^{-1} and Ca increased with increments from 0 to 1000µmol mol^{-1}.

2.3.6 Protein and chlorophyll quantification

i) Protein

Whole leaves were homogenized with a pestle in a mortar, in liquid nitrogen, and aliquots stored in eppendorf tubes at –80°C until 1ml aliquots of the homogenized powder were assayed for soluble protein content. For protein extraction, leaf tissue (1ml tobacco leaf powder) was ground in ice-cold mortars with pestles, using liquid nitrogen. When leaf tissue had been thoroughly homogenized, 1ml extraction buffer (0.1M citrate phosphate buffer, pH6.5) was added and samples further homogenised with a pestle. Homogenate was poured into an eppendorf tube, and the mortar and pestle rinsed with an additional 1ml extraction buffer which was added to the same tube. Samples were centrifuged at 12 000rpm for 10min at 4ºC, and protein content of supernatant determined.

In general, protein content of extracts was determined according to the method described by Bradford (1976). Plant extracts (5µl) were diluted with water to a volume of 800µl before the addition of Bradford colour reagent (200µl; Bio-Rad, UK) to give a final volume of 1ml. The reaction solution was incubated at room temperature for 30 min, after which the absorbance of the solution was determined on a spectrophotometer at a wavelength of 595nm. Values were compared to a bovine serum albumin (BSA) standard consisting of 0, 1, 2, 5, 10, 15, or 20µg BSA in diluted Bradford colour reagent (20%, v/v), which was also incubated and measured as described above. All measurements were done in duplicate.

ii) Chlorophyll

Whole leaves were homogenized with a pestle in a mortar, in liquid nitrogen, and aliquots stored in eppendorf tubes at –80°C until 1ml aliquots of the homogenized powder were assayed for chlorophyll content. Chlorophyll content was determined according to the method of Lichtenhaler and Wellburn (1983). Leaf tissue (1ml tobacco leaf powder) was first ground in an ice-cold mortar with a pestle, using liquid nitrogen. 1ml ice-cold acetone (80%) was added and leaf tissue further homogenised. Homogenate was decanted into an eppendorf tube, and mortar and pestle rinsed with an additional 1ml ice-cold acetone, which was added to the same tube. All samples were incubated at -20°C over night in the dark for complete chlorophyll extraction, before centrifuging at 14 500rpm for 5min at room temperature. Samples (50µl) were diluted with acetone (80%) before absorbance

was measured using a quartz cuvette in a spectrophotometer at wavelengths of 645nm and 663nm. Chlorophyll (mg l^{-1}) was calculated using the equation: chlorophyll (mg l^{-1}) = 20.2 x A_{645} + 8.02 x A_{663}.

2.3.7 RuBisCO activity and activation state

RuBisCO activity and activation state was measured by P.D.R. van Heerden (University of Pretoria). Leaf discs were collected with a freeze clamp (cooled in liquid nitrogen) from fully expanded leaves of OC-I transformed (OCE) and wild type plants at the start of the experiment (day 0) and again following seven days of growth at 26/20°C or 26/5°C. At the end of the experiment, leaf discs were also collected from young expanding leaves that developed during the 7-day treatment period. Sampling occurred 4h after the start of the light period under full illumination. Initial, total, and maximum RuBisCO activities of collected leaf samples were measured according to Keys and Parry (1990) as described by Van Heerden et al. (2003).

Leaf disks were ground in liquid nitrogen and ice cold extraction buffer (50mM Bicine/NaOH, pH 8.0; 10mM MgCl2; 1mM EDTA; 20mM DTT). RuBisCO activity was measured by incubating extract with reaction buffer containing $^{14}CO_2$ (Fig. 2.2), prepared from $NaH^{14}CO_3$ (Amersham, UK) in 100mM $NaHCO_3$, with a specific activity of 0.5 µci µmol^{-1}, and activating the reaction with Mg^{2+} and CO_2. Initial activity was measured by adding 100 µl of extract to a scintillation vial containing 900 µl reaction buffer consisting of 50mM Bicine (pH 8.0), 10mM $MgCl_2$, 10mM $NaH^{14}CO_3$ (0.5 µci µmol^{-1}), and 33mM ribulose-1,5-bisphosphate (RuBP; Sigma, UK). Reactions were stopped after 1 min by addition of 1ml of formic acid (10M). Total activity was measured after pre-incubation of extract with 1M $NaH^{12}CO_3$ for 10min at room temperature prior to starting the reaction with RuBP. Acidified samples were dried in an oven at 60ºC and resuspended in 5ml of a scintillation fluid (cocktail T, BDH Laboratory Supplies, UK). ^{14}C incorporation was measured by scintillation counting against $^{14}CO_2$ standards.

Initial activity represents the activity of the enzyme under the growth conditions at the time of sampling, without activating all available reactive sites or removing tight-binding inhibitors. Total activity is measured as the activity obtained after all available reactive sites have been activated with bicarbonate, and maximum activity is obtained by

activation of the extracted enzyme with bicarbonate after removal of all known tight-binding inhibitors.

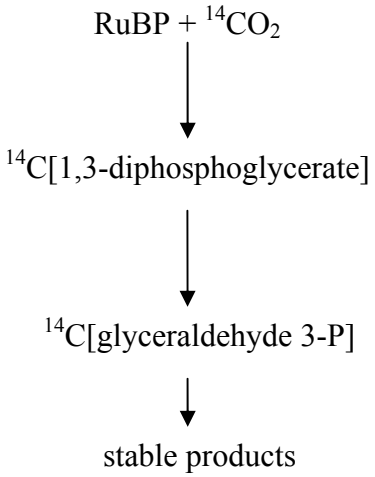

Figure 2.2 Determination of RuBisCO activity by incorporation of ^{14}C into acid stable products.

2.3.8 Western blot analysis

For the immunodetection of OC-I, RuBisCO, and RuBisCO activase in tobacco leaves, leaf discs were extracted in buffer containing 50mM Tris-HCl (pH7.8), 1mM EDTA, 3mM DTT, 6mM PMSF and 30mg insoluble PVPP. Proteins were separated by standard SDS-PAGE procedures according to the method described by Sambrook et al. (1989). Generally, 10-50µg of total soluble protein of crude leaf extracts was separated for analysis. Samples were first incubated at 95°C for 5min in loading buffer containing 62.5mM Tris-HCl (pH 6.8), SDS (2%, w/v), glycerol (10%, v/v), β-mercaptoethanol (5%, v/v) and bromophenol blue (0.001%, w/v), and then loaded onto a precast SDS-PAGE gel (10%) (BioRad, UK). Electrophoresis was performed at 100V through the stacking gel and 120-180V through the resolving gel until the blue front of the loading dye reached the bottom of the gel.

Proteins were transferred to nitrocellulose membranes (Hybond C-extra, Amersham Pharmacia Biotech, UK) in a BioRad Mini protein II transfer apparatus filled with transfer buffer (Sambrook et al., 1989), at 4ºC and 60V for 40min. After transfer, the membrane was incubated in a 5% fat free milk powder/TBS buffer (blocking buffer) over night at 4°C with shaking to prevent non-specific binding of primary antibody. Incubation with

primary antibody occurred in blocking buffer for 2-4h at room temperature with shaking. Concentrations of primary antibodies (polyclonal and raised in rabbit) were as follows: OC-I - 1:5 000, RuBisCO - 1:1 000, RuBisCO activase - 1:250 and glutamine synthetase - 1:500. The membrane was then washed 10-15min three times with blocking buffer before incubation with secondary antibody (1:1000 dilution for 2-4h at room temperature). Secondary antibody was horseradish peroxidase conjugated. After secondary antibody incubation, the membrane was once again washed three times for 10-15min with blocking buffer before signal detection using a buffer containing chloronaphthol (0.04%, w/v) and H_2O_2 (0.05%, v/v) in 50mM Tris (pH7.6). Membranes were incubated in detection buffer until bands could clearly be seen, and then rinsed in distilled water.

2.3.9 In situ localization of RuBisCO

In situ localization was performed by E. Olmos (CEBAS-CSIC, Murcia, Spain). For this procedure leaf samples were fixed at 4ºC in 3% paraformaldehyde and 0.25% glutaraldehyde in 0.1M phosphate buffer (pH 7.2) for 2.5h. The samples were dehydrated with a graded ethanol series and embedded in London Resin White (LR White) acrylic resin. Ultrathin sections (60-70nm) were made on a Leica EM UC6 Ultramicrotome (Leica Microsystems GMBH, Wetzlar). Ultrathin sections on coated nickel grids were incubated for 30min in PBS plus 5% (w/v) BSA to block non-specific protein binding on the sections. They were then incubated for 3h with anti-RbcL (RuBisCO Form I and Form II) antibody raised in rabbit (Agrisera, Vännäs, Sweden) diluted (1:250) in phosphate buffered saline (PBS) plus 5% (w/v) bovine serum albumin (BSA). After washing with PBS plus 1% (w/v) BSA, the sections were incubated for 1.5h with the secondary antibody goat anti-rabbit IgG gold labelled (10nm, British BioCell International) diluted 1:50 with PBS plus 1% (w/v) BSA and 1% (w/v) Goat Serum (Sigma). The sections were washed sequentially with PBS (two washes) and distilled water (five washes). Ultrathin sections were poststained with uranyl acetate followed by lead citrate and observed in Philips Tecnai 12 transmission electron microscope.

2.3.10 Proteolytic activity detection in plant extracts

Cysteine protease activity was detected in plant extracts using a synthetic substrate specific for cysteine proteases (cathepsin B/L) according to a Barret (1980) with slight modifications. In a microtitre plate well, total soluble protein (25µg) was diluted to a final

volume of 100µl by the addition of buffer (0.1M citrate phosphate buffer pH6 with 5mM DTT, 1mM EDTA, 0.01% CHAPS). After adding 1µl substrate (0.5% [w/v] N-CB2-phe-arg-MCA in DMSO), increase in fluorescence due to free 7-amino-4-methylcoumarin in the reaction solution was measured at 360nm for excitation and 460nm for emission in a multiwell plate reader over 30min. A control was measured containing the substrate without protein extract and subtracted from samples containing protein extract.

To measure inhibition of activity by cysteine protease inhibitors in the extracts, samples were preincubated with 100µM E64 (Sigma, UK) for 15min at 37ºC before assaying. E64 is an irreversible, potent, and highly selective inhibitor of cysteine proteases.

2.3.11 Two-dimensional (2-D) gel electrophoresis

The proteome of leaf 16 (as counted from the bottom) from either wild type or OC-I-expressing tobacco was analysed and compared by 2D electrophoresis.

i) Protein extraction and solubilisation

Proteins were extracted essentially as detailed in the handbook "2-D Electrophoresis. Principles and Methods" (GE Healthcare). Freeze-dried leaf material was ground in liquid nitrogen. Approximately 200-250mg leaf powder was incubated over night at –20°C in precipitation buffer (1ml) containing TCA (10%, w/v) and β-mercaptoethanol (0.07% v/v) in acetone (100%, v/v). Precipitated protein was pelleted by centrifuging for 25min at 4°C at 20 000xg and washed 6 times with ice cold washing buffer containing acetone (90%, v/v) and β-mercaptoethanol (0.07% v/v) in Milli-Q water. Proteins were solubilised in sample buffer (1ml) containing urea (8M), CHAPS (2%, w/v), DTT (9.3mg l^{-1}), and IPG buffer pH3-10 (0.5%, v/v) (GE Healthcare) by sonication in an ultrasonic water bath for 1 hour, while vortexing at 15 min intervals. Afterwards, samples were incubated in a heating block for 1.5h at 30°C with vortexing at 15 min intervals. Tubes were further incubated at room temperature overnight for optimal protein solubilisation. Cell debris was removed by centrifugation for 25min at 20 000xg. Solubilised proteins were quantified using the Bradford assay and ovalbumin (Sigma) as standard.

Protein content of samples was determined as described previously (chapters 2-4) except that samples and standards were neutralised with 0.1N HCl to a final concentration of

0.001N (Ramagli, 1999) before measurement. Neutralisation of samples and standards corrects for the effects of basic reagents (8M urea) present in solubilisation buffer that affect the binding of Coomassie G-250 dye to proteins. In this case, ovalbumin (Sigma) was used as standard instead of BSA, since BSA can absorb twice as much dye as most other proteins, which might cause an underestimation of the actual amount of protein being assayed.

ii) First dimension electrophoresis

After protein extraction (as described above), samples were diluted in sample buffer containing a few grains bromophenol blue to a concentration of 0.6µg μl^{-1}. Isoelectric focusing was performed on 150µg protein using Immobiline DryStrip immobilised pH gradient (IPG) strips (13cm) (GE Healthcare) and the Ettan IPGphor apparatus (GE Healthcare), with voltage being increased stepwise as follows: 30V (12h; for rehydration of strip), 100V (1h), 500V (1h), 1000V (1h), 5000V (1h), and 8000V (19 000 Vh) to obtain a total of 26 000Vh. IPG strips were then incubated for 15min each in equilibration buffer (6M urea, 50mM Tris-HCl pH8.8, 30% v/v glycerol, 2% w/v SDS, a few grains bromophenol blue) containing DTT (10mg ml^{-1}) to preserve the fully reduced state of denatured, unalkylated proteins, followed by similar incubation in equilibration buffer containing iodoacetamide (25mg ml^{-1}) for the alkylation of thiol groups on proteins, to prevent their reoxidation during electrophoresis.

iii) Second dimension electrophoresis and protein fixing

Second dimension focusing of proteins was performed by SDS-PAGE on a 1mm, 12% resolving gel with migration at 25mA/gel for 20min followed by 30mA/gel for approximately 4h or until the blue dye front had reached the bottom of the gel. Proteins were fixed in the gel overnight by incubation in fixing solution (50% methanol, v/v, 10% acetic acid, v/v) on a rocking platform at low speed.

iv) Gel staining and image analysis

After fixing of protein, gels were rinsed 3x in Milli-Q water before being stained for 24h in GelCode Blue (Pierce) on a rocking platform at low speed. Gels were rinsed 3x in Milli-Q water before being scanned for image analysis. Images were captured using the

ImageMaster Labscan software, and analysed using Phoretix 2D Expression v2005 software.

2.3.12 Spot identification

Spots of interest were excised from polyacrylamide gels after 2-D electrophoresis for peptide fingerprint analysis by surface-enhanced laser desorption ionization - time of flight mass spectrometry (SELDI-TOF MS) or mass spectrometry mass spectrometry (MS/MS). MS/MS was performed on excised spots at the McGill Proteomics Platform (McGill University, Montreal, Quebec) using an ESI-Quad-TOF mass spectrometer. For SELDI-TOF MS the procedure according to Jensen et al (1999) was followed.

Spots were excised and washed with water/acetonitrile (1:1, v/v) 2x15min. Liquid was removed and replaced with 20µl acetonitrile until gel pieces became white and stuck together. Gel pieces were then rehydrated in 0.1M NH_4HCO_3. An equal volume of acetonitrile was added and the sample incubated for 15min before drying down in a vacuum centrifuge. Gel particles were then swollen in a solution containing 10mM DTT and 0.1M NH_4CO_3 for 45min at 56°C to reduce the protein. The liquid was replaced with 50mM iodoacetamide, 0.1M NH_4CO_3 and the samples incubated for 30min at room temperature in the dark for alkylation of proteins. Liquid was removed and the samples dried in a vacuum centrifuge. In-gel digestion was performed by adding 10µL digestion buffer (50mM NH_4CO_3, 5mM $CaCl_2$) containing trypsin (20ng μl^{-1}) and incubating for 45min on ice. The remaining enzyme supernatant was removed and replaced with digestion buffer (without trypsin, to prevent autodigestion of trypsin).

Samples were then incubated over night at 37°C before peptides were extracted from the gel pieces. For aqueous extraction 20µl NH_4HCO_3 (25mM) was added and samples incubated for 15min in an ultrasonic water bath at 37°C. The same volume of acetonitrile was added, and the incubation step repeated. The supernatant from this step was recovered. For organic extraction 40µl of acetonitrile: TFA (2%) (1:1, v/v) was added to the gel particles. Samples were incubated for 15min in an ultrasonic water bath at 37°C. This step was repeated once and the supernatants pooled. Supernatant was dried down to 1-2µl, after which samples were redissolved in 5µl of a solution containing acetonitrile (5%) and TFA (0.1%).

Samples (1-2µL) were then spotted onto an H4 ProteinChip array (which has a chromatographic surface) (Ciphergen) and mixed with α-cyano-4-hydroxycinnamic acid (CHCA) [20%; in acetonitrile (5%)/TFA (0.1%)]. CHCA is an energy absorbing molecule that allows the efficient laser desorption and ionization of small proteins (< 15kDa). Samples were then analysed by surface-enhanced laser desorption/ionization – time of flight/mass spectrometry (SELDI-TOF/MS) in the Ciphergen SELDI-TOF mass spectrometer (GE Healthcare). Spectra were calibrated against CHCA peaks (643.360Da, 1059.5Da, and 1475.48Da). Peptide peaks with a signal to noise ratio >5 were identified using the Ciphergen ProteinChip Software v3.2.0, and used to identify proteins with the Mascot search engine (www.matrixscience.com; Perkins et al., 1999). The type of search performed was a peptide mass fingerprint search at the NCBInr database as on 15 June 2007 (*Viridiplantae* only), with trypsin as enzyme, carbamidomethyl (C) as fixed modification, oxidation (M) as variable modification, using average mass values, a peptide mass tolerance of ± 1Da, and a maximum of one missed cleavage. MS/MS results were obtained from the McGill proteomics portal online (http://portal.proteomics.mcgill.ca/portal). An MS/MS ion search was performed using the Mascot search engine and a database containing all available nucleotide sequences as on 5 January 2007 in order to find protein homologs, with search specifications of trypsin as enzyme, carbamidomethyl (C) as fixed modification, oxidation (M) as variable modification, using monoisotopic mass values, a peptide mass tolerance and fragment mass tolerance of ± 0.5Da, and maximum of one missed cleavage.

2.3.13 Statistical methods

The data was statistically analysed using parametric tests at a stringency of $P < 0.05$. The significance of variation in mean values for growth parameters and pigment and protein determinations was determined using a T-test. The significance of the data for immuno-gold labelling measurements was analysed using ANOVA and Tukey HSD tests.

2.4 Results

It has previously been shown that expression of OC-I in transgenic tobacco plants decreased plant growth and development rates and protected photosynthesis from chilling-induced inhibition (Van der Vyver et al., 2003). These effects were documented in three independent transgenic lines compared to the wild type and empty vector controls

confirming that the slower developments growth and delayed senescence traits are very likelylinked to the expression of the transgene as was the protection of photosynthesis from chilling induced inhibition (Van der Vyver et al., 2003). Since Van der Vyver et al. (2003) demonstrated unequivocally that the altered traits under investigation are related to the expression of the transgene, the mechanisms by which altered leaf CP activity influences leaf protein composition, photosynthesis, RuBisCO protein content and activity, leaf and plant senescence in one transgenic line (line T4/5) compared to wild type untransformed controls was studied here (with specific focus on proteins involved in photosynthesis).

2.4.1 Leaf protein composition and turnover

To determine whether leaf protein composition was modified in the OCE plants, leaf proteins were extracted from the youngest mature leaves (number 16) of 10 week-old control and OCE plants and separated using 2-D gel electrophoresis (Fig. 2.3). Leaf proteins were extracted and precipitated by standard proteomic procedures, in which the RuBisCO large subunit (LSU) has only limited solubility (Ramagli, 1999). Since RuBisCO generally accounts for 30 to 60% of total soluble proteins in the leaves of C_3 species, it is important to use this selective procedure in order to limit the amount of the RuBisCO LSU on the gels so that other proteins of lower abundance are not obscured. The Phoretix 2D gel analysis software identified 765 protein spots in the extracts prepared from control leaves and 860 protein spots in extracts from OCE leaves. Key parameters (spot volume, pI and MW) were calculated for all spots by the software. Fifty one spots were chosen for more intensive characterisation based on visible differences in spot volume. Of the 51 spots, 13 were not statistically different in volume between C and OCE plants, 7 spots had significantly greater volume in C plants, 26 spots had significantly greater volume in OCE plants, 2 spots were below the level of detection in OCE plants and 3 spots were only detected in OCE plants (Supplementary Table 1 on CD).

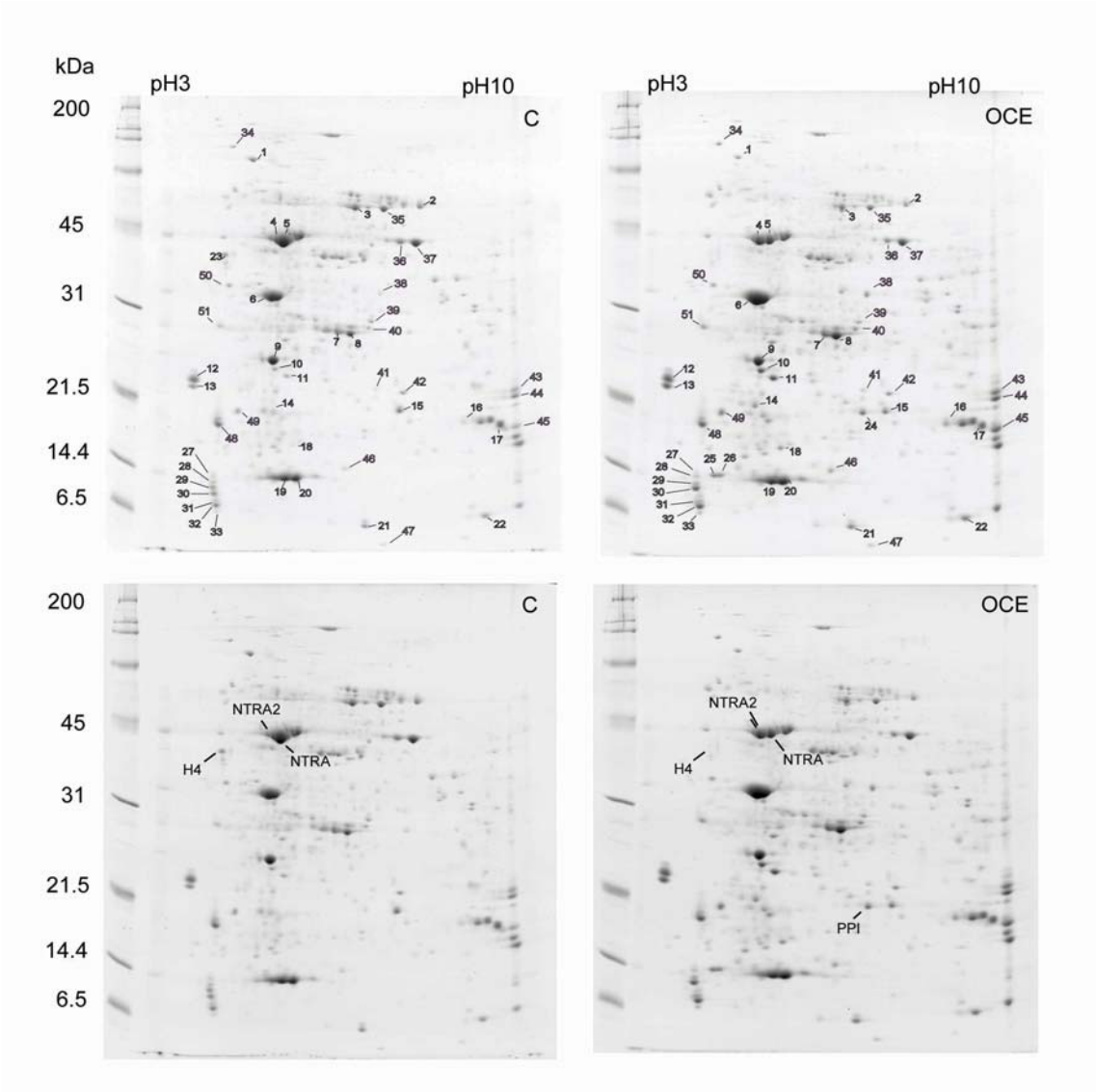

Figure 2.3. The effect of inhibition of CP activity in OCE leaf protein abundance and composition. Proteins were extracted from leaf 16 of control and OCE plants at 8 weeks and were separated on bi-dimensional gels. Proteins with major differences in abundance are indicated (1-51) in upper panels. The position of the proteins with the greatest differences: two rubisco activase forms (NTRA and NTRA2), histone 4 (H4) and putative pepyidylprolyl isomerise (PPI) are indicated in the lower panels.

Two spots showing a difference in volume (Fig. 2.3 upper panels, spots 4 and 5) were identified using SELDI-TOF MS. These proteins were highly homologous to RuBisCO activase 2 (accession Q40565) (spot 4) and RuBisCO activase (accession 1909374A) (spot 5) (Table 1). Spot 4 also showed significant homology to RuBisCO activase (accession 1909374A) and RuBisCO activase 1 (accession Q40460), while spot 5 showed significant homology to RuBisCO activase 1 (accession Q40460) and RuBisCO activase 2 (accession Q40565). The normalised volumes for spots 4 and 5 in OCE extracts were respectively

2.42 and 2.99 times greater than those found in C extracts. In OCE protein extracts, spot 4 had a larger volume than spot 5 (1.3 times).

To further characterise the RuBisCO activase isoforms present in these studies, alignments were performed with three GenBank tobacco RuBisCO activase sequences and two Arabidopsis RuBisCO activase isoforms (Table 1; Supplementary Fig. 1). While the highest scores for spots 4 and 5 were RuBisCO activase 2 and RuBisCO activase from tobacco, the comparison with Arabidopsis revealed the absence of the C-terminal amino acids characteristic of the long isoform of this gene in Arabidopsis. Instead of the final 36 C-terminal amino acids present in the long Arabidopsis isoform, the Arabidopsis short isoform has only 8 amino acids (TEEKEPSK: Werneke et al., 1989), a difference that is considered to result from alternative splicing. The Arabidopsis large isoform has a MW of 46kDa while the small isoform is approximately 43kDa. Spot 4 has the highest homology to NTRA2 (RA2, Supplementary Fig. 1) which lacks the C-terminal amino acids FAS. Spot 5 had the highest homology to another identified tobacco RuBisCO activase (1909374A, RuAct, Supplementary Fig. 1). This form lacks the first 59 amino acids in the N-terminus and also contains 3 additional amino acids at the C-terminal (FAS) when compared to RA2. Spot 5 also shows high homology with NTRA1 (RA1, Supplementary Fig. 1) which has the full-length N-terminal sequence but also has the extra amino acids at the C-terminal. Spot number 23 on Fig. 2.3 upper panels has very low abundance in the OCE proteome (Supplementary Table 1) and was identified by LC-MS/MS analysis as highly homologous to volvox histone H4 (P08436), histone H2A.3 from wheat (HSWT93) and rice H2A protein (AAF07182) (Table 1). Spot number 24 in the OCE proteome, which is below detection in C extracts, was identified by LC-MS/MS and was significantly homologous to rice Os05g0103200 (NP_001054392), which is described as a chloroplast precursor of peptidyl-prolyl cis-trans isomerase TLP20 (EC 5.2.1.8). This protein contains a cyclophilin ABH-like region. Spot 24 is also significantly homologous to an Arabidopsis peptidylprolyl isomerase-like protein (CAC05440), which also has a strong similarity to the chloroplast stromal cyclophilin, ROC4.

Table 2.1. Identification of protein spots showing different abundance in control and OCE lines after 2D electrophoresis. Peptide fingerprint analysis (NTRA2 and NTRA) and/or ion analysis (H4 and PPI) using the Mascot search engine was used to establish protein identities.

Spot	Identification method	Accession	Protein name	Score	e-value	Queries matched	Peptide Sequence (MS/MS)
NTRA2 (4)	SELDI-TOF MS	Q40565	RuBisCO activase 2 (RA 2)	98	6.80E-05	9	
		1909374A	RuBisCO activase	75	1.30E-02	8	
		Q40460	RuBisCO activase 1 (RA 1)	71	3.30E-02	8	
NTRA (5)	SELDI-TOF MS	1909374A	RuBisCO activase	117	7.70E-07	15	
		Q40460	RuBisCO activase 1 (RA 1)	108	6.10E-06	15	
		Q40565	RuBisCO activase 2 (RA 2)	94	1.40E-04	13	
H4 (23)	MS/MS	P08436	Histone H4	195		3	ISGLIYEETR DNIQGITKPAIR TVTAMDVVYALK
		HSWT93	histone H2A.3	48		1	AGLQFPVGR
		AAF07182	H2A protein	48		1	AGIQFPVGR
PPI (24)	MS/MS	NP_001054392	Os05g0103200	357		16	TFKDENFK DFMIQGGDFDK VYFDISIGNPVGK HVVFGQVIEGMDIVK DFMIQGGDFDKGNGTGGK
		CAC05440	peptidylprolyl isomerase-like protein	105		7	TFKDENFK

The relative abundance of the RuBisCO LSU and RuBisCO activase proteins was determined in leaves at different positions on the stem of 14 week-old plants (Fig. 2.4) using western blot analysis.

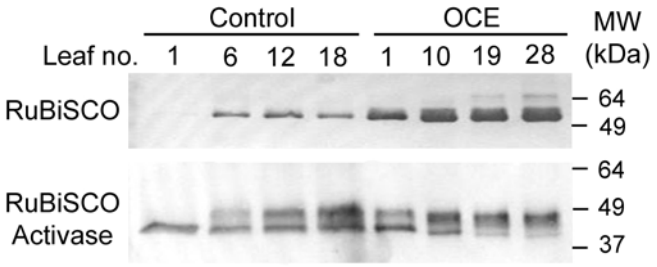

Figure 2.4 Western blot analysis of the abundance of the RuBisCO large subunit, and RuBisCO activase in leaves at different positions on the stem of 14 week-old plants. Soluble proteins were extracted from leaves at the positions on the stems as indicted, with Leaf No 1 being at the bottom of each plant and leaf 18 or 28 being the youngest mature leaf on the control and OCE plants respectively. 10µg and 30µg aliquots of leaf protein were loaded per well for the detection of RuBisCO and RuBisCO activase proteins, respectively.

In the control plants, the amount of RuBisCO LSU protein was highest in the mature source leaves and least abundant in the youngest (18) and oldest (1) leaves (Fig. 2.4). However, the relative abundance of the RuBisCO LSU protein was much higher in the leaves of the OCE plants at all ranks on the stem, even in the oldest leaves (Fig. 2.4). A development-dependent difference in the RuBisCO activase protein bands was also observed (Fig. 2.4). Two distinct bands of RuBisCO activase protein were observed on Western blots using specific antibodies in all but the oldest senescent leaves of the control plants where only the lower band was the dominant band (Fig. 2.4). In marked contrast, the higher molecular weight band of RuBisCO activase protein was more intense than the lower molecular weight band in the young leaves of OCE plants in all leaves except the oldest senescent leaf (Fig. 2.4).

2.4.2 RuBisCO degradation and leaf CP activity

To determine whether tobacco RuBisCO is susceptible to degradation by endogenous tobacco CPs we conducted *in vitro* assays comparing RuBisCO degradation in OCE extracts with that in C extracts in the absence or presence of the CP inhibitor, E64 (Fig. 2.5 A). RuBisCO was protected from degradation by endogenous CPs in OCE extracts compared to control extracts; an effect that could be mimicked by inclusion of the CP inhibitor, E64 in the assays of the control extracts (Fig. 2.5 A).

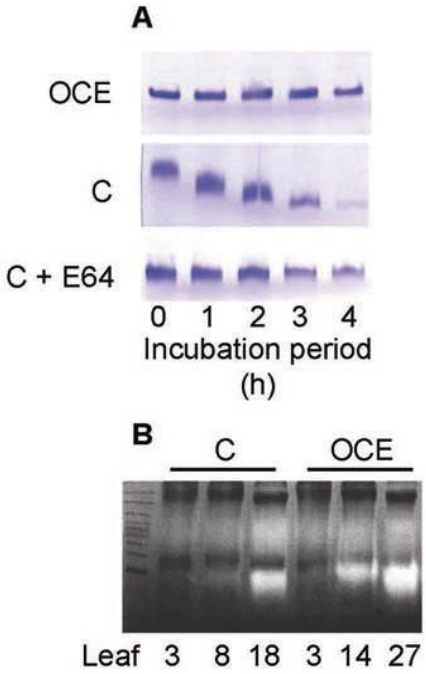

Figure 2.5 Protection of RuBisCO from degradation by OC-I in OCE plants and by E64 in control (C) plants *in vitro* assays. (A) The abundance of the RuBisCO holoenzyme protein was detected in soluble protein extracts from 4-week old control (C) and OCE plants on non-denaturing PAGE gels stained with Commassie brilliant blue. (B) In-gel activity assay showing degradation of the gelatine substrate by endogenous proteases from extracts of leaves of 14 week-old OCE and control (C) plants. Extracts were prepared from leaves at the bottom (3), middle (8, 14), and top (18, 27) leaf ranks. Equal amounts of soluble protein (40 µg per well) extracted from C and OCE plants were compared in all instances.

The protease activities of leaf extracts, scrutinised by activity staining after SDS-PAGE, revealed that the youngest leaves on OCE plants had much higher CP activities than the youngest leaves from controls (Fig. 2.5 B). This increased activity represents unknown proteases, but could include CPs. In this case, increased protease activity observed in OCE plants after separation of OC-I and the proteases they inhibit by SDS-PAGE implicate a possible feedback modulation of CP expression that enhances CP production when activity is impaired by constitutive cystatin expression.

2.4.3 Natural senescence and chilling-dependent inhibition of photosynthesis, decreased RuBisCO content and activity

It was previously shown that chilling dependent effects on photosynthesis were comparable in three independent transgenic lines relative to the wild type and empty vector controls and that effect of constitutive OC-I expression on parameters such as the CO_2 saturated rates of photosynthesis (J_{max}) and carboxylation efficiency (CE) were linked

to expression of the transgene (Van der Vyver et al., 2003). Leaf CE and J_{max} values attained maximal values two weeks after emergence in both OCE and control plants (Table 2.2). To investigate the effect of decreased CP activity on leaf senescence as determined by the age dependent decrease in photosynthesis, leaf CE and J_{max} values were measured on the same leaves from 2 to 6 weeks (Table 2.2). The OCE leaves had greater CE and J_{max} values than controls at equivalent stages of development. Moreover, the senescence-related decline in photosynthesis was delayed in the OCE leaves (Table 2.2).

Table 2.2 Senescence-related decreases in carboxylation efficiency (CE) and CO_2 saturated rates of photosynthesis (J_{max}) in wild type controls (C) and OCE tobacco leaves. Measured CE and J_{max} values, which were highest in both lines two weeks after leaf emergence, were measured in the same leaves for up to six weeks. The values represent the means ± SE of four replicates per experiment.

Time after leaf emergence (weeks)	C plants CE (mol m^{-2} s^{-1})	OCE plants CE (mol m^{-2} s^{-1})	C plants J_{max} (µmol m^{-2} s^{-1})	OCE plants J_{max} (µmol m^{-2} s^{-1})
2	0.078 ± 0.004	0.107 ± 0.007	20.3 ± 1.0	23.2 ± 0.8
3	0.069 ± 0.004	0.110 ± 0.013	15.1 ± 1.0*	21.7 ± 1.1
4	0.040 ± 0.004**	0.064 ± 0.002**	13.6 ± 1.3**	18.5 ± 1.7*
5	0.034 ± 0.004**	0.063 ± 0.005**	9.6 ± 0.6**	16.6 ± 0.6**
6	0.014 ± 0.001**	0.045 ± 0.003**	3.1 ± 0.6**	11.9 ± 0.1**

* and ** indicate significant differences at $P < 0.05$ and $P < 0.01$ respectively

Photosynthesis (Fig. 2.6 A), extractable RuBisCO activities and activation states (Fig. 2.6 B) were compared in the leaves of 6-week old plants maintained at either optimal growth temperatures or exposed to seven consecutive nights of chilling. At the beginning of the experiment (day 0), fully expanded leaves of control (Fig. 2.6 A upper panel) and OCE plants (Fig. 2.6 A lower panel) grown at optimal temperatures had very similar rates of photosynthesis.

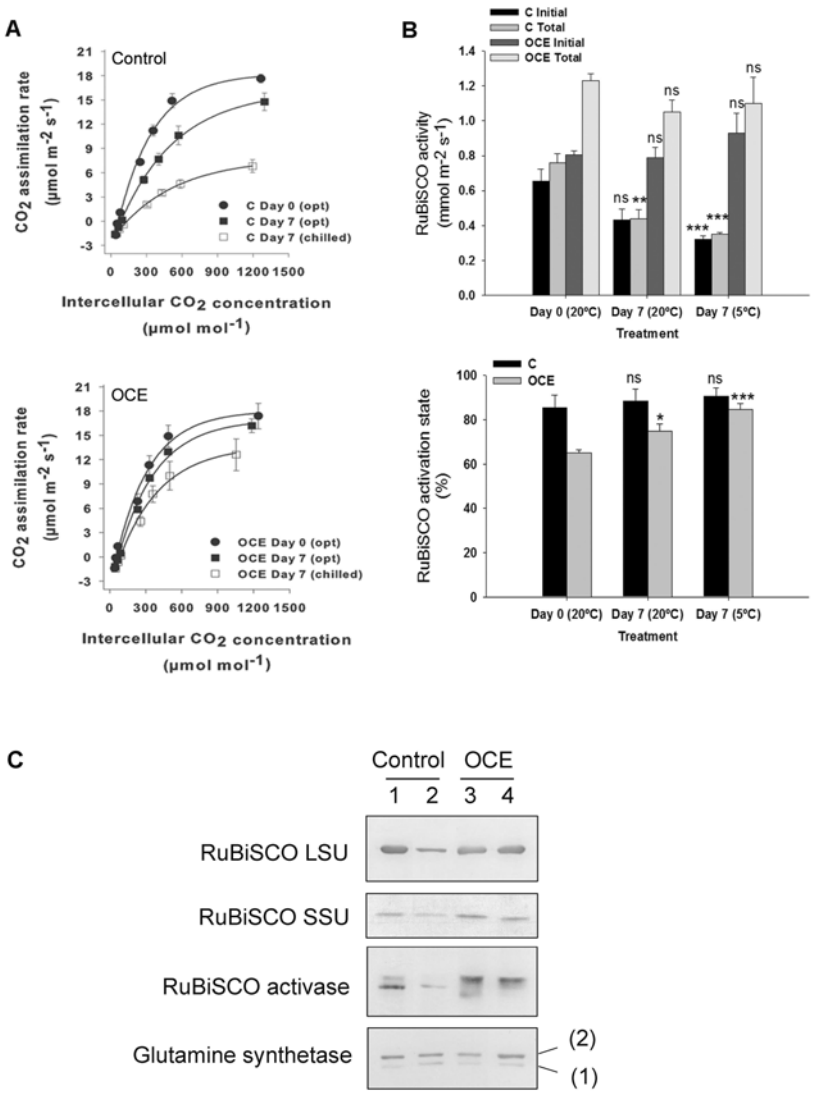

Figure 2.6 Effects of dark chilling on photosynthesis, RuBisCO activity and activation state and relative abundance of RuBisCO, RuBisCO activase and glutamine synthetase in the leaves of 6 week-old OCE and control tobacco plants. CO_2 response curves for photosynthesis (A) in control and OCE leaves were measured at day 1 (closed circle), after 7 days of growth under optimal conditions (Opt: closed square) and after 7 nights of dark chilling (Chilled; open square). Initial and total RuBisCO activities and the RuBisCO activation state in control and OCE leaves measured at day 1, after 7 days of growth under optimal conditions and after 7 nights of dark chilling (B). Immuno-detection of RuBisCO, RuBisCO activase, and glutamine synthetase (C) in soluble protein extracts from control and OCE leaves at the beginning of the experiment (lanes 1 and 3) and after 7 nights of dark chilling (lanes 2 and 4).

At this stage the OCE plants had higher total RuBisCO activities but lower activation states than controls (Fig. 2.6 B). Seven days later, the control leaves maintained at optimal temperatures had about 20% lower photosynthetic rates than the OCE plants (Fig. 2.6 A). Over the same period, total RuBisCO activity in the control leaves maintained at optimal

temperatures had also decreased (Fig. 2.6 B) with significant effect on RuBisCO activation state (Fig. 2.6 B). While RuBisCO activities were similar in OCE plants at both time points the RuBisCO activation state was slightly increased at day 7 (Fig. 2.6 B). The chilling-dependent increase in RuBisCO activation state in the OCE lines is surprising given that the overall rate of photosynthesis declined and that the initial slope of the photosynthesis: intercellular CO_2 response is also slightly decreased. However, these effects are very small compared to the large effect of chilling on photosynthesis rates in the control line, where RuBisCO activation state is unchanged. It was previously shown that the leaves of the different independent OCE lines contain about 20% more total soluble protein than those of controls at 6 weeks old (Van der Vyver et al., 2003). Consistent with this observation, the amounts of RuBisCO LSU and SSU proteins (Fig. 2.6 C) were similar in the leaves 6-week old control and OCE plants at this stage. However, dark chilling stress led to a pronounced decrease in the abundance of RuBisCO LSU and SSU proteins (Fig. 2.6 C) in the leaves of control plants. In contrast, dark chilling had no effect on the amount of detectable RuBisCO LSU and SSU proteins in the OCE plants.

2.4.4 Intracellular localisation of RuBisCO protein in chloroplasts and vesicular bodies in the palisade cells of young leaves

Electron microscopy and immuno-gold labelling with specific polyclonal antibodies to the RuBisCO LSU were used to determine the intracellular distribution of the RuBisCO protein in the youngest mature leaves of control and OCE tobacco at 6 weeks old (Fig. 2.7). Label was detected in the chloroplasts of the palisade cells of control (Fig. 2.7 B) and OCE leaves (Fig. 2.7 C). In addition RuBisCO protein was also observed in vesicular bodies outside the chloroplast (Fig. 2.7 B and C). The relative amounts of label were quantified in the chloroplasts and in the RuBisCO vesicular bodies (RVB) of both control and OCE leave (Table 2.3). No differences were observed in the relative localization of RuBisCO protein in the chloroplasts relative to the RVB's of both control and OCE leaves (Table 2.3).

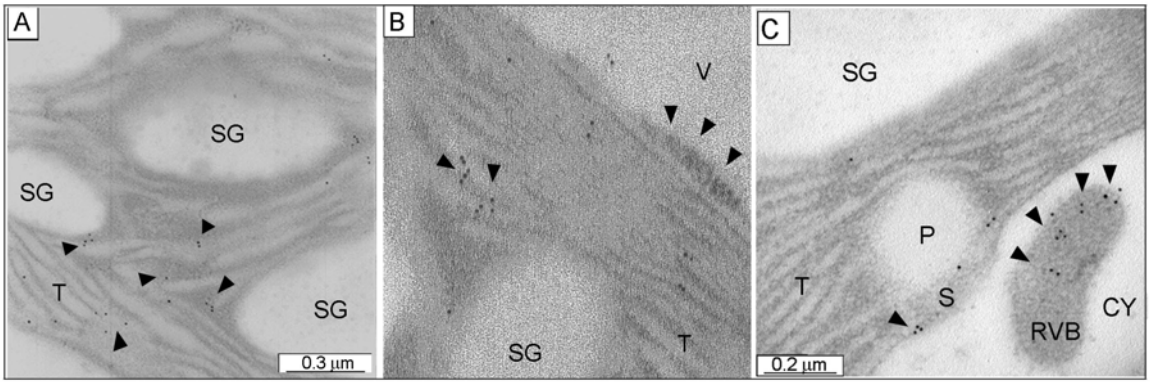

Figure 2.7 Immunogold labelling detection of RuBisCO protein in palisade cells of 6-week old control and OCE tobacco leaves. High magnification of a cross-section of a control leaf showing the structure of the palisade cells with immuno-gold labelling (A), and higher magnification images of the intra-cellular structure showing the compartmention of the label in wild type and OCE leaves (B and C). The presence of RuBisCO protein in chloroplasts and vesicular bodies outside the chloroplast is indicated in B and C Areas of immuno-gold are indicated by black arrows. CY, cytosol, IS, intercellular space; P, plastoglobulus, RVB, RuBisCO vesicle body, S, stroma, SG, starch grain, T, thylakoid membranes, V, vacuole.

Table 2.3. Counts of gold particles (GP) after immunogold labelling of RuBisCO large subunit in ultrathin leaf sections of C and OCE tobacco. Gold particles were counted in chloroplasts, RuBisCO protein vesicles (RVB) and cytosol. Values obtained were compared to controls lacking antibody (Control).

	GP in Chloroplast (μm^{-2})	*GP in RVB* (μm^{-2})	*GP in Cytosol* (μm^{-2})
Control	0.4± 0.2	0.2 ± 0.1	0.4± 0.2
OCE	27.9± 3.3*	31.4 ± 6.5*	1.4 ±0.8
C	26.7± 2.8*	29.1 ± 5.3*	1.4 ± 0.7

Mean values ± SE (n=30). The means were compared by analysis of variance and by using the Tukey multiple range test at $P < 0.05$. Significant differences between treatments are indicated by *.

2.4.5 Intracellular localisation of OC-I protein in the cytosol, chloroplasts and vacuoles in the palisade cells of young leaves

Electron microscopy and immuno-gold labelling with specific polyclonal antibodies to the OC-I protein were used to determine the intracellular distribution of the OC-I protein in the youngest mature leaves of control and OCE tobacco at 6 weeks old (Fig. 2.8). The OC-I protein was mainly located in the cytosol which had the highest relative gold particle concentrations (71 ± 8 μm^{-2}; n=9). However, label was also detected in the vacuole at a much lower gold particle concentration of 5.5 ± 2 μm^{-2} (n=9), and also in the chloroplasts

which had a gold particle concentration of 20.6 ± 4.2 μm^{-2} (n=9). Interestingly, the chloroplasts that showed immuno-gold labelling for the presence of the OC-I protein also had an alteration to the structure at the periphery of the chloroplast either beneath or adjacent to the chloroplast envelope (Fig. 2.8 A and C). A higher magnification of the chloroplast periphery shows that this is possibly fibrillar or membranous. (Fig. 2.8 B and D). Since these samples were not fixed with osmium, lipids are not stained in these images, implying that the changes in the periphery of the chloroplast is not due to changes in the lipid membrane, or that it may have a low lipid content. The chloroplasts containing changes in the structure of their periphery clearly show label (Fig. 2.8 B inset and D inset) but further studies are required to explain the presence and possible function of OC-I in the altered chloroplast periphery. Some of the OCE cells also show the presence of cytosolic inclusion bodies (Fig. 2.8 E and F), which has a crystalline structure that also contains OC-I label (Fig. 2.8 G). The high level of label in the cytosol (Fig. 2.8 H inset and I inset) is consistent with the mode of expression of the OC-I protein in these studies, where the protein lacked sequences for specific organellar targeting. However, presence of OC-I in the vacuole and chloroplast require reconfirmation and further investigation.

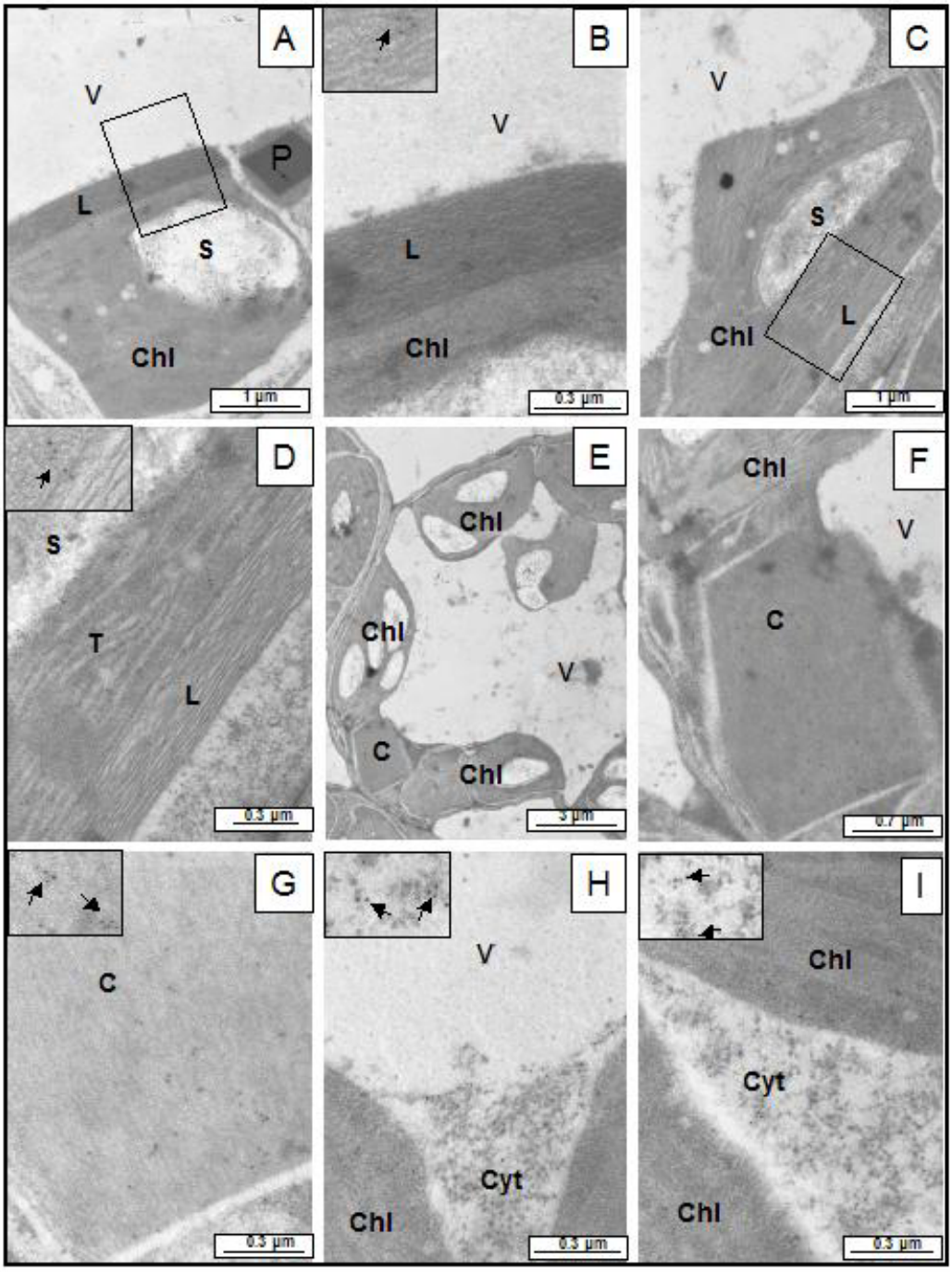

Figure 2.8 Transmission electron micrographs of immuno-gold labelling detection of OC-I protein in the palisade cells of 6-week old control and OCE tobacco leaves. Chloroplasts in OCE leaves with an unusual fibril structure below the chloroplast envelope (A and C); Enhanced images of the unusual structure below the chloroplast envelope (B and D). In both cases the chloroplasts (A and C) show labelling for OC-I protein (B and D). A section of the OCE leaf shows the presence of a cystatin inclusion body (E) together with a higher magnification image showing that the cystatin inclusion body is present in the cytosol (F) and has a crystalline structure with positive labelling for the OC-I protein (G). The presence of immuno-gold label in the cytosol of the OCE leaves (H and I). C= cystatin inclusion body; Chl, chloroplast; Cyt, cytosol; L, unusual chloroplast structure; S, starch; T, thylakoid; V, vacuole.

2.4.6 Inhibition of CP activity effects on lifespan and leaf protein and chlorophyll contents after flowering

The OCE plants have a slow growth phenotype compared to wild type or empty vector controls (Van der Vyver et al., 2003). In the present experiments, the control plants flowered at 58.33 ± 1.20 days, at which point vegetative growth ceased. The OCE plants also sustained vegetative growth until flowering but in this case vegetative development ceased at 80.67 ± 1.45 days (Fig. 2.9). Hence, at the point where the OCE lines reached sexual maturity (14 weeks in the OCE lines) the OCE lines were much taller (Fig. 2.9 A), with greater numbers of larger and heavier leaves than the controls (Fig. 2.9 B-H).

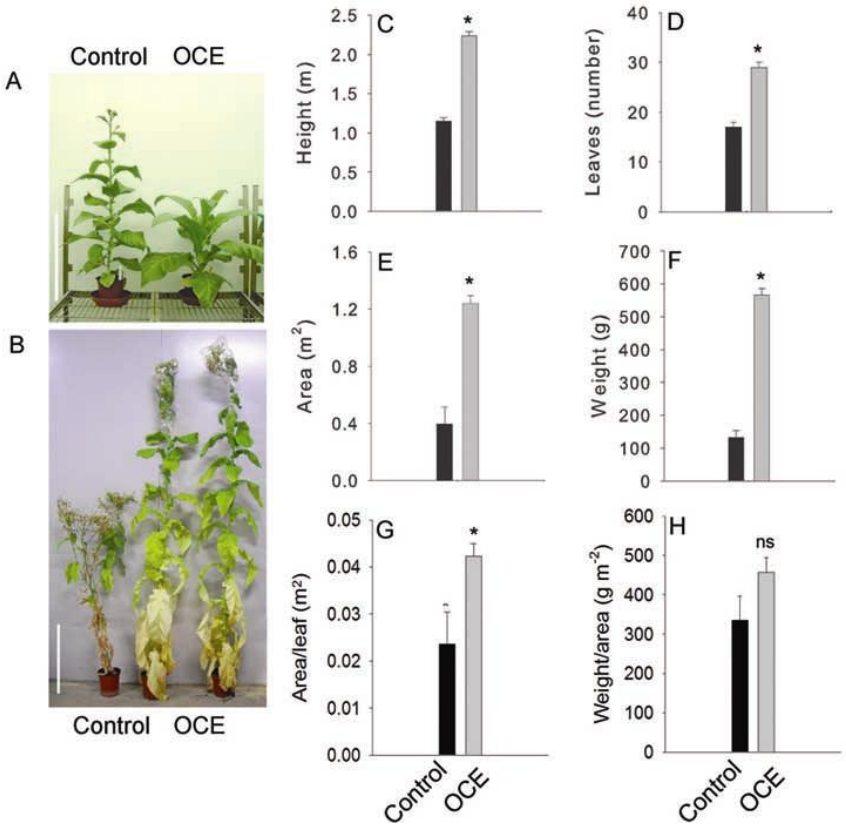

Figure 2.9. A comparison of plant growth and development in OCE and control plants. Plant phenotype at 8 weeks (A) and 14 weeks (B). After both genotypes had flowered at 14 weeks the following parameters were measured: plant height C), leaf number (D), total leaf area (E), leaf weight (F), area per leaf (G), and leaf weight per leaf area (H). Data represent average ± SE of n=6. The size bar indicates 0.5m. Significant differences at $P < 0.05$ indicated by *.

The effects of inhibition of CP activity on leaf protein accumulation were much more pronounced in 14-weeks (Fig. 2.10 A) than they were in 6-8 week-old tobacco plants (Van der Vyver et al., 2003). The increase in leaf protein in OCE plants that had flowered depended on the position on the stem (Fig. 2.10 A). Chlorophyll was also increased but

only in the youngest tobacco leaves (Fig. 2.10 B). Maximal extractable leaf CP activities were greatly decreased in OCE leaves compared to controls at all positions on the stem (Fig. 2.10 C), suggesting that the OC-I remains bound to the CP during the extraction and spectrophotometric assay procedures, whereas it is removed by the in-gel assay methods of used in Fig. 2.5 B.

Figure 8

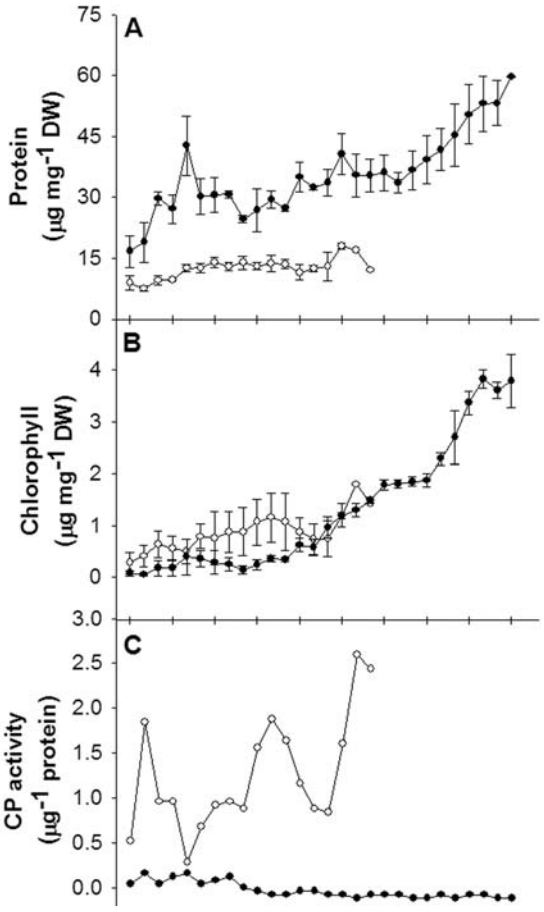

Figure 2.10. Leaf soluble protein and chlorophyll contents and cysteine protease activities in mature OCE and control tobacco plants. Soluble protein content (A). Chlorophyll content (B). Cysteine protease (CP) activity (C). Open and closed symbols represent control and OCE plants respectively.

2.5 Discussion

The results presented here demonstrate that chloroplast proteins particularly RuBisCO and RuBisCO activase are affected by the expression of an exogenous CP inhibitor. This could be due to effects of OC-I on the activity of endogenous CPs, since RuBisCO was found to be sensitive to degradation by proteases *in vitro*, a process that could be inhibited by CP

inhibitors or exogenously expressed OC-I in an in vitro study. However, for RuBisCO to be degraded by CPs *in planta*, a mechanism of interaction between RuBisco and vacuolar or vesicular CPs must exist. This would provide a link between the protein turnover machinery in the chloroplasts, cytosol and vacuoles. A detailed discussion of the results and logic corroborating the above conclusions is provided below.

While there are relatively few reports on tobacco leaf proteomics in the literature (Cooper et al., 2003; Franceschetti et al., 2004; Giri et al., 2006), the technique has been used successfully to study the proteome of leaf plasma membranes (Rouquié et al., 1997), trichomes (Amme et al., 2005) and apoplast (Dani et al., 2005). Proteome information is available for tobacco BY2 cell suspension cultures (Laukens et al., 2004) and for plastids isolated from these cultures **(**Baginsky et al., 2004). RuBisCO activase sequences (Q40565, CAA78703, or 1909374A), have been identified previously in *Nicotiana attenuata* leaves (Giri et al., 2006). In this study concerning proteins elicited by oral secretions from *Manduca sexta* seven spots with homology to RuBisCO activase were identified (Giri et al., 2006). Of these, four spots had kDa/pI values similar to reported RCA proteins, with comparable molecular weights but different pI values. In the present study, spots four and five in Fig. 2.3 occupy similar positions to the RuBisCO activase spots reported by Giri et al. (2006). Differences in the positions of the RuBisCO activase spots on the gels might arise from proteolytic cleavage (Giri et al., 2006). The data presented in Figs. 2.3-2.5 not only implicates CPs in RuBisCO activase degradation but also in the relative abundance of different forms of the protein present in leaves. The relative abundance of the two RuBisCO activase protein bands detected on Western blots was changed by inhibition of CP activity, with greater abundance of the higher molecular weight form. RuBisCO activase is a crucial regulator of RuBisCO activation state (Zhang et al, 2002). This nuclear-encoded chloroplast protein consists of two isoforms in Arabidopsis, produced by alternative splicing (Zhang et al., 2002). In Arabidopsis, the longer isoform houses critical cysteine residues that are modulated by redox changes in the stroma, particularly under limiting light intensities (Zhang et al., 2002). However, the tobacco RuBisCO activase spots examined in the present study lack the critical cysteine residues that characterise the longer isoform sequence in Arabidopsis. In order to clarify this result, further research needs to be done on the sequence of RuBisCO activase protein sequences as well as the mRNAs that encode them, in order to identify whether the two bands observed with the Western blot are isoforms or degradation produts.

While the mechanisms of turnover and degradation of RuBisCO activase remain poorly characterised, there have been a large number of studies on the turnover of RuBisCO and glutamine synthetase. Within the chloroplast oxidation of critical cysteine residues enhances the binding of the RuBisCO protein to the chloroplast envelope membranes, marking the protein for degradation (Marín-Navarro and Moreno, 2006). While chaperone-mediated autophagy pathways for oxidatively modified proteins remain 562 to be demonstrated in plants, stress-induced non-specific autophagasitic pathways of protein degradation have been described (Xiong et al., 2007). Once outside the chloroplast RuBisCO occurs in the vesicular transport system and involves cytoplasmic vacuole-type compartments (Chiba et al., 2003). Thereafter, RuBisCO degradation products appear in the vacuoles (Huffaker, 1990). While this process has only previously been considered to be important in senescing leaves where chloroplast lysis occurs (Mae et al., 1984; Ono et al., 1995; Hörtensteiner and Feller, 2002), the data presented here in Table 2.2 and Fig. 2.7 show that they are present even in young leaves. Our immo-gold labelling results demonstrate the existence of a cytoplasmic vacuole-type compartment that has been called RuBisCO vesicular bodies (RVBs) that are involved in RuBisCO degradation even in young leaves.

Since OC-I is detected both in the cytosol and the chloroplast, interaction between OC-I, endogenous protease, and RuBisCO could occur in either of these compartments. The endogenous protease inhibited by OC-I is most likely a cysteine protease or cysteine proteases that are suggested to be present in the vacuole, or small lytic vacuoles in the cytosol. Therefore a model is proposed for RuBisCO degradation of the type illustrated in Fig. 2.11 where vesicles containing CPs continuously interact with those from functional chloroplasts to remove proteins marked for degradation. RuBisCO protein is present in vesicles as well as in the chloroplasts in both young wild type and OCE leaves (Fig. 2.7, Table 2.3).

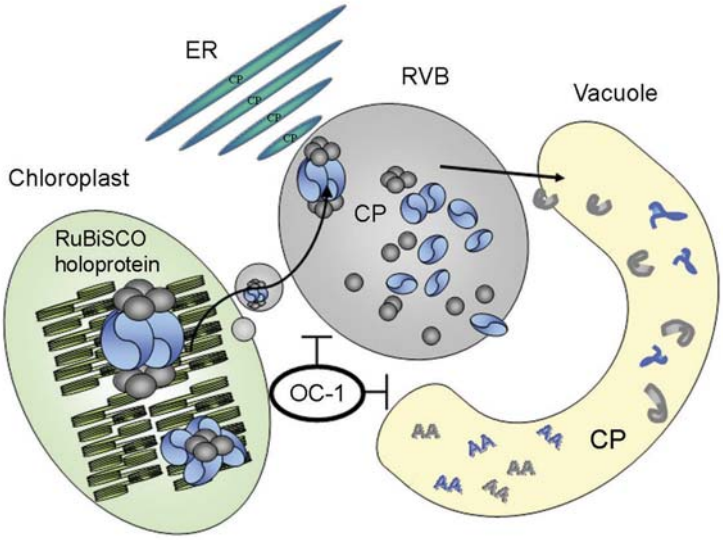

Figure 2.11 A hypothetical model for RuBisCO degradation via autophagy and the plant vesicle trafficking system. AA: amino acids; CP, cysteine protease, ER: endoplasmic reticulum; OC-I, oryzacyctatin-1.

Interestingly, RVBs have been recently shown to arise from the stromules that are continuously produced by chloroplasts even in young leaves (Ishida et al., 2007). While the function of stromules remains a matter of debate (Foyer and Noctor, 2007), available evidence suggests that stromules forge associations between chloroplasts and other organelles including the vacuole. The similar pattern of RuBisCO labelling in the RVBs and chloroplasts observed in the present study is entirely consistent with the chloroplast-stromule origin of RVBs. Furtermore, sjnce the fibrillar structure observed on the chloroplast periphery contains OC-I protein, this may provide a means by which RuBisCO and OC-I proteins are enclosed in vesicles that bud off from the chloroplast, and then fuses with a lytic vacuole in the cytosol. Plant cells contain several different types of vacuole-like compartments with distinct functions (Chrispeels and Herman, 2000). Vesicle trafficking has been traditionally viewed as a housekeeping process, but recent findings in plant, yeast and animal cells show that it can also play an important role in stress responses (Chrispeels and Herman, 2000; Herman and Schmidt, 2004). The physiological and biochemical identity of vacuoles is largely determined by correct targeting of vesicles and their cargo (Vitale and Pedrazzini, 2005).

While the data presented here concerning RVBs are limited to RuBisCO, it may be that other chloroplast proteins such as RuBisCO activase are also present in the RVB's. This aspect is currently under investigation together with the role of CPs and cystatins in the

formation of peripheral structure adjacent to the chloroplast envelope that we have observed when CP activity is inhibited. To date we have only counted the number of RVB's in the leaves of young plants prior to flowering, and values appear to be similar regardless of leaf CP activity. However, the number may increase as the leaf develops and senesces. Despite the absence of this information at present, our data suggest that the RuBisCO turnover cycle involving RVB's must have a feedback interaction with the chloroplast that requires CP activity, as inhibition of CPs by expression of an exogenous cystatin allows the chloroplast to maintain RuBisCO activity and photosynthesis upon exposure to stress. These interactions may be controlled by redox regulation.

The data presented here show that the lifespan of tobacco plants can be extended by the expression of an exogenous phytocystatin. It is unusual for a single transgene to have such a large effect on plants, however, and it is also possible that the observed morphological changes may be due to somaclonal variation. However, the large effect may be caused by OC-I inhibiting endogenous cysteine proteases that play key roles in the synthesis of developmentally important hormones. In order to clarify this, the level of developmentally important hormones in these plants could be measured.

```
RA1             MATSVSTIGAVNKTPLSLNNSVAGT-SVPSTAFFGKTLKKVYGKGVSSPKVTNKSLRIVA
RA2             MATSVSTIGAANKAPLSLNNSVAGT-SVPSTAFFGKTLKKVYGKGVSSPKVTNRSLRIAA
RuAct           ------------------------------------------------------------
AthL            MAAAVSTVGAINRAPLSLNGSGSGAVSAPASTFLGKKVVTV-SRFAQSNKKSNGSFKVLA
AthS            MAAAVSTVGAINRAPLSLNGSGSGAVSAPASTFLGKKVVTV-SRFAQSNKKSNGSFKVLA

RA1             EQIDVDPKKQTDSDRWKGLVQDFSDDQQDITRGKGMVDSLFQAPTGTGTHHAVLQSYEYV
RA2             EEKDADPKKQTYSDRWKGLVQDFSDDQQDIARGKGMVDSLFQAPTGTGTHHAVLQSYEYV
RuAct           EEKDADPKKQTDSDRWKGLVQDFSDDQQDITRGKGMVDSLFQAPTGTGTHHAVLQSYEYV
AthL            VKED----KQTDGDRWRGLAYDTSDDQQDITRGKGMVDSVFQAPMGTGTHHAVLSSYEYV
AthS            VKED----KQTDGDRWRGLAYDTSDDQQDITRGKGMVDSVFQAPMGTGTHHAVLSSYEYV
                 : *    *** .***:**. * *******:********:**** *********.*****

RA1             SQGLRQYNLDNKLDGFYIAPAFMDKLVVHITKNFLKLPNIKVPLILGIWGGKGQGKSFQC
RA2             SQGLRQYNMDNTLDGFYIAPSFMDKLVVHITKNFLKLPNIKVPLILGVWGGKGQGKSFQC
RuAct           SQGLRQYNLDNKLDGFYIAPAFMDKLVVHITKNFLKLPNIKVPLILGIWGGKGQGKSFQC
AthL            SQGLRQYNLDNMMDGFYIAPAFMDKLVVHITKNFLTLPNIKVPLILGIWGGKGQGKSFQC
AthS            SQGLRQYNLDNMMDGFYIAPAFMDKLVVHITKNFLTLPNIKVPLILGIWGGKGQGKSFQC
                ********:** :*******:***************.***********:************

RA1             ELVFRKMGINPIMMSAGELESGNAGEPAKLIRQRYREAAEIIRKGNMCCLFINDLDAGAG
RA2             ELVFRKMGINPIMMSAGELESGNAGEPAKLIRQRYREAAEIIRKGNICCLFINDLDAGAG
RuAct           ELVFRKMGINPIMMSAGELESGNAGEPAKLIRQRYREAAEIIRKGNMCCLFINDLDAGAG
AthL            ELVMAKMGINPIMMSAGELESGNAGEPAKLIRQRYREAADLIKKGKMCCLFINDLDAGAG
AthS            ELVMAKMGINPIMMSAGELESGNAGEPAKLIRQRYREAADLIKKGKMCCLFINDLDAGAG
                ***: ***********************************::*:**::*************

RA1             RMGGTTQYTVNNQMVNATLMNIADNPTNVQLPGMYNKQENARVPIIVTGNDFSTLYAPLI
RA2             RMGGTTQYTVNNQMVNATLMNIADNPTNVQLPGMYNKQENARVPIIVTGNDFSTLYAPLI
RuAct           RMGGTTQYTVNNQMVNATLMNIADNPTNVQLPGMYNKQENARVPIIVTGNDFSTLYAPLI
AthL            RMGGTTQYTVNNQMVNATLMNIADNPTNVQLPGMYNKEENARVPIICTGNDFSTLYAPLI
AthS            RMGGTTQYTVNNQMVNATLMNIADNPTNVQLPGMYNKEENARVPIICTGNDFSTLYAPLI
                ************************************:******** *************

RA1             RDGRMEKFYWAPTREDRIGVCTGIFRTDNVPAEDVVKIVDNFPGQSIDFFGALRARVYDD
RA2             RDGRMEKFYWAPTREDRIGVCKGIFRTDNVPEEAVIKIVDTFPGQSIDFFGALRARVYDD
RuAct           RDGRMEKFYWAPTREDRIGVCTGIFRTDNVPAEDVVKIVDNFPGQSIDFFGALRARVYDD
AthL            RDGRMEKFYWAPTREDRIGVCKGIFRTDKIKDEDIVTLVDQFPGQSIDFFGALRARVYDD
AthS            RDGRMEKFYWAPTREDRIGVCKGIFRTDKIKDEDIVTLVDQFPGQSIDFFGALRARVYDD
                ********************.******::  * ::.:** ******************

RA1             EVRKWVSGTGIEKIGDKLLNSFDGPPTFEQPKMTIEKLLEYGNMLVQEQENVKRVQLADK
RA2             EVRKWVSGTGIEAIGDKLLNSFDGPPTFEQPKMTVEKLLEYGNMLVQEQENVKRVQLAET
RuAct           EVRKWVSGTGIEKIGDKLLNSFDGPPTFEQPKMTIEKLLEYGNMLVQEQENVKRVQLADK
AthL            EVRKFVESLGVEKIGKRLVNSREGPPVFEQPEMTYEKLMEYGNMLVMEQENVKRVQLAET
AthS            EVRKFVESLGVEKIGKRLVNSREGPPVFEQPEMTYEKLMEYGNMLVMEQENVKRVQLAET
                ****:*.. *:* **.:*:** :***.****:** ***:******* ***********:.

RA1             YLKEAALGDANADAINNGSFFAS-----------------------------------
RA2             YLKEAALGDANADAINTGNF-------------------------------------
RuAct           YLKEAALGDANADAINNGSFFAS-----------------------------------
AthL            YLSQAALGDANADAIGRGTFYGKGAQQVNLPVPEGCTDPVAENFDPTARSDDGTCVYNF
AthS            YLSQAALGDANADAIGRGTFYGK----------------TEEKEPSK-----------
                **.:***********. *.*
```

Supplementary Figure 1. Pair-wise alignment of RuBiSCO activase isoforms from Arabidopsis and three RuBiSCO activase proteins identified in tobacco. RA1 - RuBiSCO activase 1 (tobacco), RA2 - RuBiSCO activase 2 (tobacco), RuAct - RuBiSCO activase (tobacco), AthL - RuBiSCO activase long isoform (Arabidopsis), AthS - RuBiSCO activase short isoform (Arabidopsis).

Consensus symbols:
* - all residues in the column are identical in all sequences in the alignment
: - conserved substitutions are observed
. - semi-conserved substitutions are observed